Mat. Res. Soc. Symp. Proc. Vol. 674 © 2001 Materials Research Society

Magnetic Properties and Scaling Behavior in Perovskite–like $La_{0.7}(Ba_{1-x}Pb_x)_{0.3}CoO_3$ System

Chiung-Hsiung Chen, Ting-Sheng Huang and Ming-Fong Tai
Department of Physics, Chung Cheng University,
160 San-Hsing, Ming-Hsiung, Chia-Yi 621, Taiwan.

ABSTRACT

In this study, we used x-ray diffraction patterns and *dc* magnetic measurements to investigate the crystallographic structure, magnetic properties and scaling behavior of the distorted perovskite $La_{0.7}(Ba_{1-x}Pb_x)_{0.3}CoO_3$ ($0 \le x \le 0.5$) system with a constant ratio of Co^{4+}/Co^{3+}. Samples with $x = 0.0$ and 0.1 were crystallized in the cubic structure with $a \sim 7.76$ Å whereas samples with $x \ge 0.2$ were crystallized in an orthorhombic *Pbnm* space group with $a \sim b \sim 5.50$ Å and $c \sim 7.85$ Å. For all our samples the spin-glass-like behavior were observed in low temperature and low field ranges. The Pb^{2+} substitution on Ba^{2+} site does not significantly affect the ferromagnetic transition temperature T_C, but does introduce large variation in the magnetic strength. In both the ferromagnetic and paramagnetic states the minimum values of the average effective moments provided by every Co ion occur at $x = 0.3$. We also observed the scaling behaviors of magnetic data in all samples. The derived values of the critical exponents (β, γ, δ) were consistent with those predicted by mean field theory and a three-dimensional Heisenberg model.

INTRODUCTION

The discoveries of high-T_c superconductivity in cuprates and great magnetoresistance (MR) in manganates have initiated intensive investigations of the $(La_{1-x}A_x)TO_3$ compounds (A = Ca, Sr, Ba, Pb; T = *3d* transition metal) [1-3]. In the Co-based perovskite-like oxides the competition between the crystal-field splitting and the intra-atomic Hund's coupling of Co ions lead to a variety of magnetic and electronic phase transitions among the high-, intermediate- and low-spin configurations of Co^{3+} and Co^{4+} ions. The $(La_{1-x}A_x)CoO_3$ system also displays many new and unusual behaviors open to study. Such as orbital and charge ordering phenomena as well as large changes in the electrical, magnetic, and structural properties, driven by small variations of composition, temperature, magnetic field, or pressure. However, many of these properties are still not understood completely.

In some transition-metal oxides, such as Tl- and Bi-based high-T_c superconducting cuprates, the addition of a small Pb amount can reduce the sintering temperatures and the process times as well as stabilize the required structures with special physical properties. In addition, because Pb ions does not contribute significant magnetic signal in solids and have very similar chemical properties to the divalent alkali earth ions, the substitution of Pb atom on the alkali earth atom can be used to study the disorder effects of chemical, orbital, charge, or magnetic moment. In this report, we investigated the substitution effect of Pb^{2+} ions for Ba^{2+} ions on the structural and magnetic properties in the distorted perovskite $La_{0.7}(Ba_{1-x}Pb_x)_{0.3}CoO_3$ ($x \le 0.5$) system with a fixed ratio of Co^{4+}/Co^{3+}. The short-range ferromagnetic order and the scaling behavior have been studied in this series.

EXPERIMENTAL DETAILS

We prepared $La_{0.7}(Ba_{1-x}Pb_x)_{0.3}CoO_3$ samples with x = 0 - 0.5 using a standard powder solid-state reaction method**.** Stoichiometric amounts of high-purity La_2O_3, $BaCO_3$, Pb_3O_4, and Co_3O_4 raw powders were homogenously mixed and completely ground. After that, the samples were fired to 1150°C and hold at the same temperature for 12 hours. The heated samples were cooled to low temperature and removed, reground, and reheated at the same temperature for an addition 24 hours. The processes were repeated at least three times until the samples are of a single-phase. The thoroughly reacted powders were pressed into pellets during the last sintered process. All heated processes were progressed at ambient atmosphere and used warm-up and cooling-down rates of 300°C/h. We collected X-ray powder diffraction (XRD) data with a MAC MPX^3 powder X-ray diffractometer using Cu $K\alpha$ radiation and a secondary graphite monochromator. A step-scan mode with a step size of $\Delta 2\theta$ = 0.002° were selected in a $2\theta/\theta$ scanning from 20° to 100° using a counting rate of 5 sec/step. We further refined all XRD patterns by using a Riqas program based on an analysis technique of the Rietveld method. *Dc* magnetic measurements were performed with an Oxford MagLab magnetometer. The zero-field cooled (ZFC) and field cooled (FC) magnetization curves were carried out under various *dc* external fields H from 0 – 5 T. Isothermal magnetic hysteresis loops at various temperatures were also obtained in applied fields of up to 5 T.

RESULTS AND DISCUSSION

We assessed the phases of all the samples by XRD patterns and all the samples were of single phase. The samples of x = 0 and 0.1 were crystallized in a cubic unit cell with a ~ 7.76 Å, whereas samples with $x \geq 0.2$ were crystallized in the orthorhombic *Pbnm* space group with a ~ 5.46 Å, b ~ 5.50 Å, c ~ 7.85 Å. The refinement results appear that all Pb ions are divalent, not tetravalent and the ratios of Co^{4+}/Co^{3+} keep at a constant value in this series. When the Ba^{2+} ions are partially substituted by the Pb^{2+} ions, only slight differences in lattice parameters, distances, and angles among the atoms induce. The results may be contributed to a small difference in the ionic radii of Pb^{2+} and Ba^{2+} ions as well as very little changes in compositions. The crystallographic refinements of all the XRD data have been reported elsewhere in details [5,6].

Figure 1 shows that the temperature dependence of FC and ZFC magnetization in H = 1 kOe for all the samples. The ferromagnetic transition temperature T_C was determined from the inflection point of the $M(T)$ curve. The remarkable feature of magnetic properties of this series is the appearance of short-range ferromagnetic interactions. This is confirmed by observing a spin-glass-like behavior in low temperature and low field ranges. In the low applied fields both the ZFC and FC magnetization curves split at temperatures below a so-called irreversibility temperature, T_r ($\leq T_C$), comparing those curves in figures 1(a) and 1(b). The irreversibility temperature decreases with increasing external field and the difference between the ZFC and FC M (T) curves in $T < T_r$ also decreases with increasing temperature and field. Both the ZFC and FC M (T) resemble substantially in the range of $T \geq T_r$ and implying the reversibility of magnetization. In addition, the low-field ZFC $M(T)$ clearly shows a sharp cusp at a so-called spin freezing (or spin-glass transition) temperature, T_g, where it attains a maximum magnetization, as demonstrated in figure 1(b). As the strength of external magnetic field increases, T_g also shifts to a lower temperature and the cusp in the ZFC $M(T)$ is smeared out to broad maximum. These

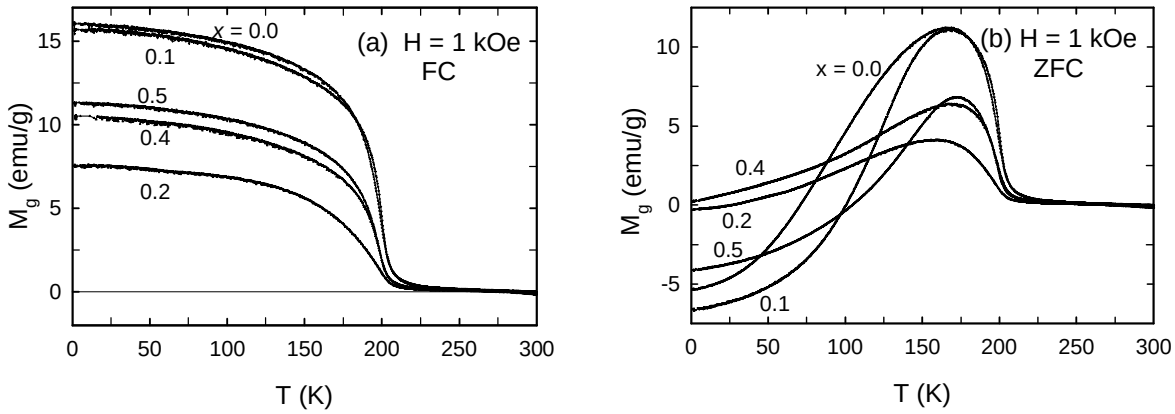

Figure 1. (a) Field-cooling and (b) zero-field-cooling magnetizations *vs* temperature in H = 1 kOe for $La_{0.7}(Ba_{1-x}Pb_x)_{0.3}CoO_3$ compounds with x = 0 - 0.5.

phenomena are identifying features of a spin glass or a glass-cluster state.

The variations of T_C, θ_p, T_g, and T_r in a fixed field with the Pb content x are displayed in figure 2. The limited changes in these characteristic temperatures were obtained as x varies from 0 to 0.5: T_C = 206 K $\pm$ 2 K, θ_p = 205 K $\pm$ 10 K, $T_g(H = 1\ \text{kOe})$ = 166 K $\pm$ 3 K and $T_r(H = 1\ \text{kOe})$ = 183 K $\pm$ 5 K for $0 \le x \le 0.5$. Although a structural phase transition occurring in $0.1 < x < 0.2$, the Pb substitution on Ba does not strongly affect those magnetic related temperatures. Thus, we propose that the major factor affecting the ferromagnetic transition temperature in this series is the ratio of Co^{4+}/Co^{3+}, not by the ratio of Pb/Ba. The ratio of the mixed-valence Co ions, which is controlled by the ratio of $(Ba^{2+} + Pb^{2+})/La^{3+}$, determines the concentration of the hole-type carriers and further impinges on the electronic and magnetic properties in these cobaltates.

The magnetization at temperatures above T_C obeys well a Curie-Weiss relation of $\chi = \chi_0 + C/(T-\theta_p)$ in our measuring fields. Here, C is the Curie constant, θ_p the paramagnetic Curie-Weiss temperature, and χ_0 the temperature-independent term of susceptibility. In this series the major contribution to the magnetization arises from the *3d* cobalt ions, very few contributions from the

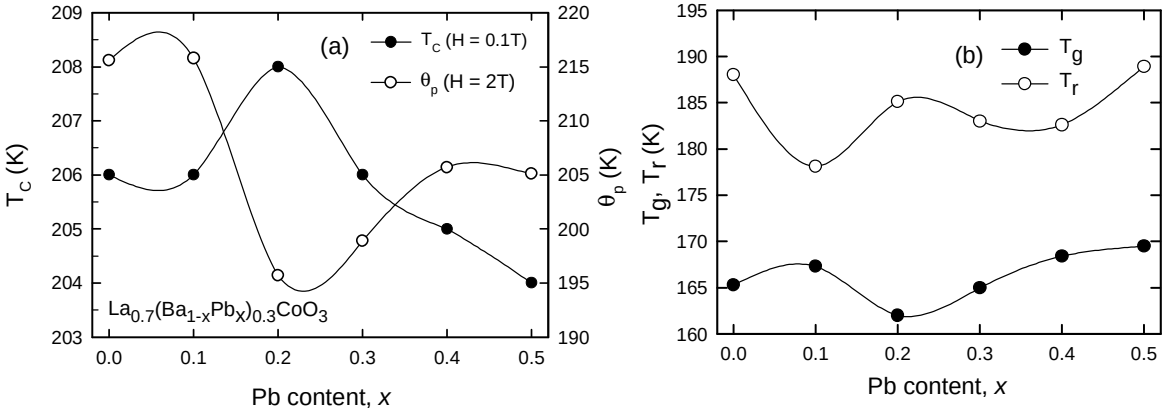

Figure 2. (a) Ferromagnetic transition temperature T_C and Curie-Weiss paramagnetic temperature θ_p versus Pb content, and (b) spin-glass transition temperature T_g and reversible temperature T_r versus Pb content for $La_{0.7}(Ba_{1-x}Pb_x)_{0.3}CoO_3$ system.

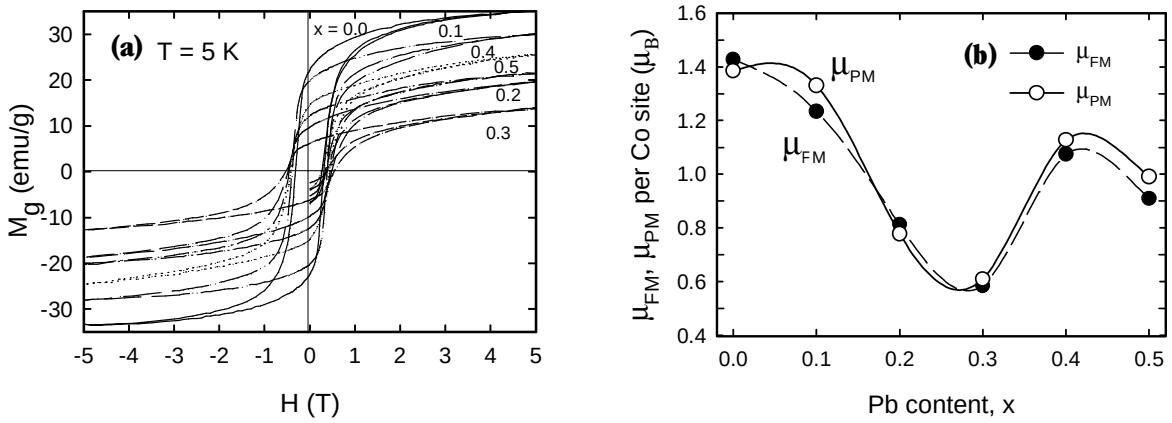

Figure 3. (a) Magnetic hysteresis loops at T = 5 K, and (b) dependence of the average effective moment per Co site in a FM and PM phase upon Pb content for $La_{0.7}(Ba_{1-x}Pb_x)_{0.3}CoO_3$ series.

other ions, even Pb and Ba ions. So the value of C is used to calculate the average effective moment per Co ions, μ_{PM}, in the paramagnetic state.

Figure 3(a) displays the magnetic hysteresis loops, $M(H)$, at T = 5 K for all our samples. The saturation magnetic moment in the low-temperature magnetic ordering phase, μ_{FM}, is estimated by the saturation magnetization in the $M(H)$ loop at low temperature (T = 5 K) or is determined by the low-temperature magnetization of the FC $M(T)$ curve in a high field (H = 4 T). As shown in figure 3(b) both μ_{PM} and μ_{FM} for each sample appear very slight difference and have the same dependence on Pb content. The μ_{PM} and μ_{FM} decrease with increasing Pb content from ~1.4 μ_B as x = 0, follow by attaining a minimum value of about 0.6 μ_B at x = 0.3, then increase as x = 0.4 and slightly decrease again as x = 0.5. We consider that the addition of Pb ions may changes the degree of chemical disorder and in advance changes the ordering of magnetic moments. As a result it may lead to the average effective magnetic moments in both ferromagnetic and paramagnetic phases to vary with the Pb concentration. The kind of the oscillating variation may be attributed to the competition between the size effect of the ionic radii and the effect of chemical and/or charge disorder. The further investigation of this variation is in progress.

In general, a well-defined equilibrium phase transition is expected to show scaling behavior. The scaling theories [1,6-9] predict that magnetic susceptibility χ (= M/H) exhibits a scaling relation as follows:

$$\chi - \chi_0 = \frac{C}{T-\theta_p}(1-q) = \frac{C}{T}[1-|t|^{\beta} f_{\pm}(H^2/|t|^{\beta+\gamma})], \quad (1)$$

$$q(t,H) = |t|^{\beta} f_{\pm}(H^2/|t|^{\beta+\gamma}), \quad (2)$$

$$q|t|^{-\beta} = f_{\pm}(H^2/|t|^{\beta+\gamma}), \quad (3)$$

In these equations t is the reduced temperature $t = (T - T_0)/T_0$ with T_0 being a certain magnetic transition temperature. The T_0 may be T_C for a FM/PM transition and may be T_g for a SG transition. The q in equations (2) and (3) is as functions of T and H. If a well-defined magnetic phase transition exits, these equations will present two different scaling functions: f_+ for $t > 0$ in a PM state and f_- for $t < 0$ in a FM/SG state, respectively. Since we did not observe a significant relaxation effect, the magnetic data are considered to be in equilibrium states for all our samples.

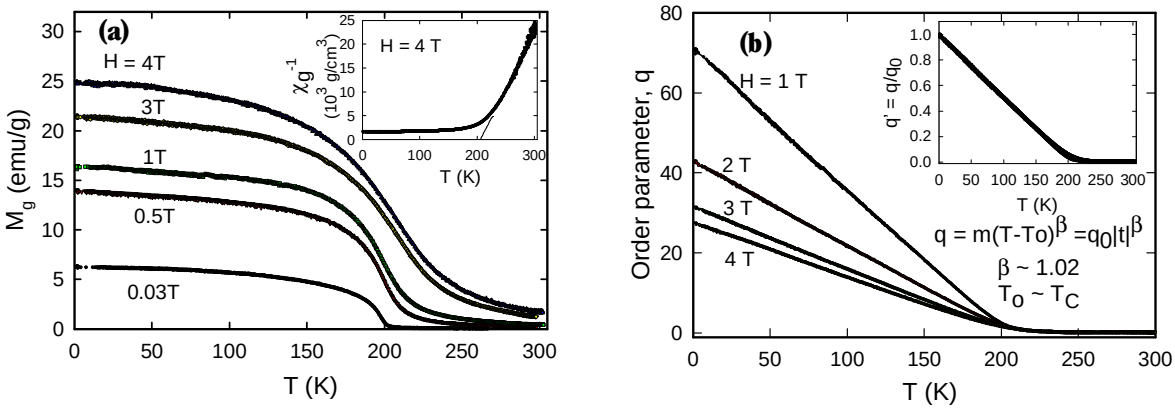

Figure 4. (a) FC magnetization versus temperature in various applied fields for the sample of $x = 0.4$. Inset plot: Inverse susceptibility versus temperature in $H = 4$ T. (b) Order parameter q as a function of temperature, T, in various fields show linear relations. Inset plot presents the temperature dependence of the normalized order parameter in all the external fields.

This behavior is observed mostly in high-quality single crystals or thin films, but scarcely in polycrystalline samples. However, all our samples present this scaling behavior. In this report, we use the sample of $x = 0.4$ as a typical example for discussing the scaling behavior in detail. The universal property of the other samples in our series has been reported elsewhere [6].

Figure 4(a) and 4(b) display the temperature dependencies of the FC magnetization and the order parameter, $M(T)$ and $q(T)$, in various external fields ranging from 0.03 to 4 T. The $q(T)$ curves are extracted from the experimental data of $\chi(T) = M(T)/H$ during the FC measurements using equation 1 and the parameters of $\theta_p = 205.7 \pm 0.3$ K, $C = 4.35\times10^{-3} \pm 3.2\times10^{-5}$ cm^3·K/g and $\chi_0 \sim 0$. The used parameters are obtained by fitting the $\chi(T)$ experimental data in $H = 4$ T to the Curie-Weiss relation $\chi_0 + C/(T-\theta_p)$ as shown in the inset plot of figure 4(a).

Obviously, figure 4(b) appears that q linearly decreases with increasing temperature in a wide low temperature and field ranges. The inset plot in figure 4(b) displays the normalized $q(T)$, *i.e.* $q'(T) = q(T)/q_0$, where q_0 is the extrapolated value of q at $T = 0$ K. For $T < T_0$, the $q'(T)$ curves for various fields all collapse to an universal straight line of $q' = |T - T_0|$. Here T_0 is considered as a certain transition temperature as described above. In general, we can also say that the order parameter well obeys a power-law relation of $q_0|t|^\beta$ with the reduced temperature $t = (T_0 - T)/T_0$. All $q(T)$ curves in various applied fields give the average fitting values of $\beta = 1.05 \pm 0.01 \sim 1$ and $T_0 = 208$ K $\pm$ 2 K. The fitting value of T_0 is very close to the value of T_C as H approaches zero. This result is consistent to the prediction of the mean-field theory in which the powder-law relation has an exponent of $\beta = 1$ and is strictly a linear relation. This result clearly confirms that the magnetic behavior of this compound in temperatures below and even close to the critical point can be described well by the mean-field theory. The same result is usually observed in some conventional spin glass systems and some strong ferromagnetic systems.

We are interested in the magnetic behavior near the critical point T_C. The field dependence of q can be calculated from the experimental $M(H)$ curves using equation 1. It also shows a power-law relation of $q = q_0' H^{2/\delta}$ in high fields. For $q(H)$ at $T = 5$ K a fitting parameter of $\delta = 2.80 \pm 0.01$ was obtained as $H > 0.3$ T. This δ value gives a critical exponent of $\gamma = 3.87 \pm 0.02$

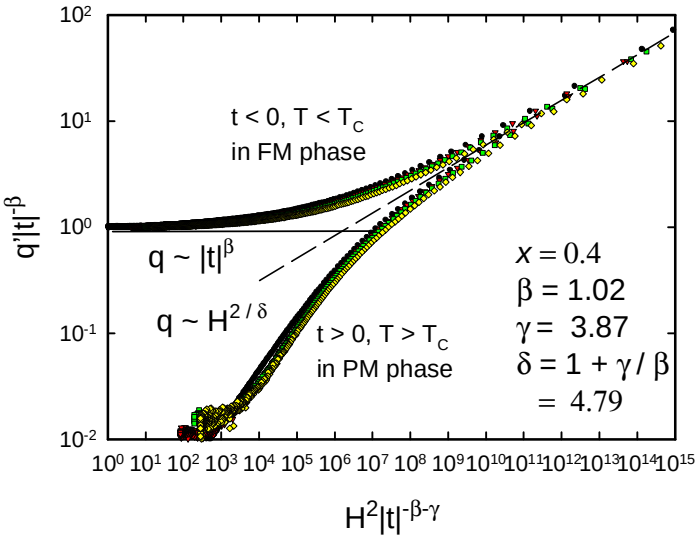

Figure 5. Log-log plot of $q'|t|^{-\beta}$ *vs* $H^2|t|^{-\beta-\gamma}$ of the sample of $x = 0.4$. All magnetic data in the ranges of $2 \leq T \leq 300$ K and $1\ \text{T} \leq H \leq 4$ T collapse to two curves f_+ for $t > 0$ and f_- for $t < 0$, which clearly demonstrates the scaling relations in equation 3.

based on the relation of $\delta = 1 + \gamma/\beta$. For demonstrating the scaling behavior, the log-log plots of $q|t|^{-\beta}$ versus $H^2|t|^{-\beta-\gamma}$ in various fields (0.03 T – 4 T) as shown in figure 5 are obtained by using the derived values of $\beta = 1.05$, $\gamma = 3.87$, and $T_0 = 208$ K. All of the q data collapse onto two curves. One is the scaling functions $f_+(x)$ for $t > 0$ ($T > T_C$, in the PM phase) and the other is $f_-(x)$ for $t < 0$ ($T < T_C$, in the FM phase). For $t < 0$, $q|t|^{-\beta}$ approaches a constant (~ 1) for small $H^2|t|^{-\beta-\gamma}$ as indicates in the dashed line in figure 5. The line of $q \sim H^{2/\delta}$ with $\delta = 2.80$ as the solid line in figure 5 demonstrates the asymptotic behavior for $T \rightarrow T_C$. The shapes of both the scaling functions are also quite similar to those observed in the most conventional ferromagnetic materials. These values of critical exponents are between those predicted by the mean field theory and those derived by a three-dimensional Heisenberg model [1, 6-9].

In summary the scaling behavior in our compounds has some approximations as follows:

(1) For high $T > T_C$ ($t > 0$), equation 1 reduces to the Curie-Weiss relation [$\chi = \chi_0 + C/(T - \theta_p)$] and q gradually approaches to zero with increasing temperature. For all our $La_{0.7}(Ba_{1-x}Pb_x)CoO_3$ samples, the value of χ_0 is so small that it can be neglected.

(2) For $T \rightarrow T_C$ or a large H , *i.e.*, $H^2|t|^{-(\beta+\gamma)} >> 1$ ($H^2 >> |t|^{(\beta+\gamma)}$), a power form of $q \sim H^{2/\delta}$ with $\delta = 1 + \gamma/\beta$ (as the dashed line in figure 5) is used to describes the field dependence of the order parameter near the magnetic transition point T_C.

(3) As temperature is far away the critical transition point T_C or $H \rightarrow 0$, the value of $H^2|t|^{-(\beta+\gamma)}$ becomes a relative small value. Thus, $q \sim |t|^{\beta}$ for $t < 0$. It means that $f_-(0)$ approaches to a nonzero constant as the solid line in figure 5. While $f_+(0)$ approaches to zero for $t > 0$ as described in the above situation.

CONCLUSIONS

The striking features of the spin glass behavior and the scaling behavior have been studied in the perovskite-like $La_{0.7}(Ba_{1-x}Pb_x)CoO_3$ oxides with x = 0 - 0.5. The Pb^{2+} substitution on Ba^{2+} ions does not significantly affect the ferromagnetic transition temperature T_C, which is determined mainly by the ratio of Co^{4+}/Co^{3+}. But the addition of Pb ions leads to a change in the chemical and magnetic disorder, and induces a large variation in the magnetic strength.

ACKNOWLEDGMENTS

This work was supported by the National Science Council, R.O.C. under the grant No. NSC-89-2112-M194-023. The authors would also like to thank Dr. Shin-Tai Chen for his critical reading of this manuscript.

REFERENCES

1. J. M. D. Coey, M. Viret and S. von Molná, *Advances in Physics* **48**, 167 (1999).
2. M. F. Tai, Y. Y. Lee and J. B. Shi, *J. Mag. Magn. Mater.* **209**, 148 (2000).
3. N. Gayathri, A. K. Raychaudhuri, S. K. Tiwary, R. Gundakaram, A. Arulraj and C. N. R. Rao, *Phys. Rev*. **B56**, 1345 (1997).
4. R. Caciuffo, D. Rinaldi, and Barucca, J. Mira, J. Rivas, M. A. Señarís-Rodríguez, P. G. Radaelli, D. Fiorani and J. C. Goodenough, *Phys. Rev*. **B59**, 1068 (1999); D. N. H. Nam, K. Jonason, P. Nordblad, N. V. Khiem and N. X. Phuc, *Phys. Rev*. **B59**, 4189 (1999).
5. C. H. Chen, T. S. H, Y. L. Shieh and M. F. Tai, submitted to *J. Mag. Magn. Mater.* (2001).
6. Chiung-Hsiung Chen, *Thesis of Master Degree*, National Chung Cheng University, Taiwan (July, 2001).
7. F. C. Chou, N. R. Belk, M. A. Kastner, and R. J. Birgeneau and A. Aharony, *Phys. Rev. Lett.* **75**, 2204 (1995); B. Barbara, A. P. Malozemoff and Y. Imry, *Phy. Rev. Lett*. **47**, 1852 (1981).
8. A. P. Malozemoff, S. E. Barnes and B. Barbara, *Phy. Rev. Lett*. **51**, 1704 (1983).
9. N. Moutis, I. Panagiotopoulos, M. Pissas, and D. Niarchos, *Phys. Rev*. **B59**, 1129 (1999).